Intensity noise behavior of an InAs/InGaAs quantum dot laser emitting on ground states and excited states

Intensity noise behaviour of an InAs/InGaAs quantum dot laser emitting on ground-state and excited-state

R. Pawlus[1], L. L. Columbo[2], P. Bardella[2], S. Breuer[1,*], and M. Gioannini[2]

[1] Institute of Applied Physics, Technische Universität Darmstadt, 64289 Darmstadt, Germany
[2] Dipartimento di Elettronica, Politecnico di Torino, 10129 Torino, Italy
[*] Corresponding author: stefan.breuer@physik.tu-darmstadt.de

Compiled June 10, 2022

We experimentally and numerically study the amplitude stability of an InAs/InGaAs quantum dot laser emitting simultaneously on ground-state (GS) and excited-state (ES) at center wavelengths 1245 nm and 1168 nm respectively. The stability is quantified by spectrally-resolved noise current analysis in dependence on the laser injection current. We find a non-monotonic behavior of the amplitude noise which shows a reduction of up to 4 dB when GS and ES emit simultaneously. Simulations based on a rate equation model confirm the reduction in noise and suggest the cascaded GS and ES carrier paths as the relevant underlying mechanism.

OCIS codes: (140.5960) Semiconductor lasers; (250.5590) Quantum-well, -wire and -dot devices;(270.2500) Fluctuations, relaxations, and noise

http://dx.doi.org/10.1364/ao.XX.XXXXXX

1. INTRODUCTION

Quantum dot (QD) lasers offer advantages including fast carrier dynamics and incomplete gain clamping [1]. Their discrete energy level structure allows simultaneous lasing at the ground state (GS) and the excited state (ES) transition.

The simultaneous GS and ES emission has been predicted in [2], and afterwards studied theoretically [3–10] and experimentally [11–17]. Both investigations focused on the two-state emission in steady-state operation of QD lasers [5, 6], on specific dynamical regimes [4, 13, 18] and on passive mode locking [7, 14, 19, 20]. Antiphase fluctuations of the GS and ES output power in the time domain have been reported for InAs/InP QD lasers in [21] and for InAs/GaAs QD lasers in [22]. The coupling between GS and ES emission trough carriers has been identified as the origin of such a particular dynamical behavior [23]. A similar dynamics has also been observed in the competition between different longitudinal modes in single-state QD lasers [24], leading to a constant total output power.

The intensity noise behavior has been extensively studied in QD lasers emitting at 1.3 µm in [25–27] and at 1.55 µm in [28, 29].

In this work, we investigate the spectrally-resolved amplitude noise of a two-state emitting QD laser both, from the experimental and theoretical point of view.

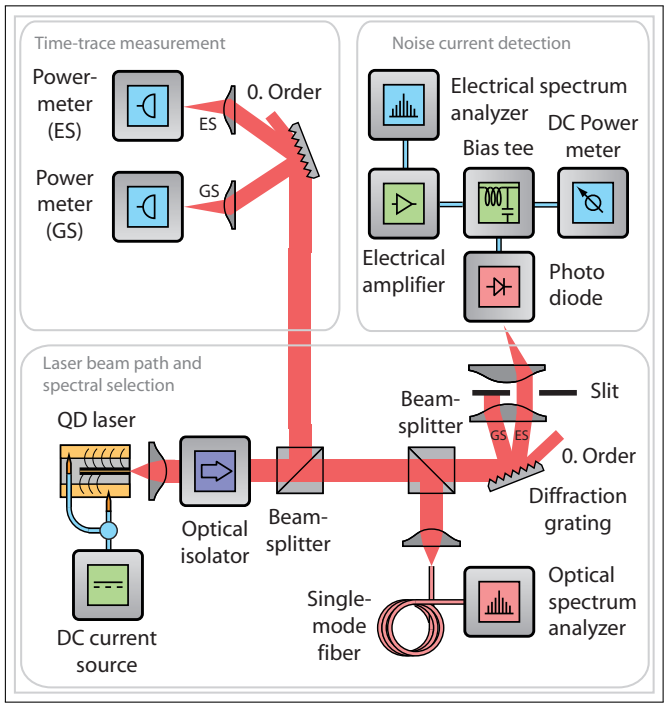

Fig. 1. Schematic of the experimental set-up depicting the QD laser, the beam path and the spectral selection of GS and ES (bottom), the noise current analysis (top, right) and the time-resolved AC output power (top, left). The set-up is built within a noise shielded box.

2. LASER, SETUP AND NOISE QUANTIFICATION

We consider a QD laser whose active region consists of 5 layers of InAs/InGaAs QDs embedded in a 440 nm GaAs waveguide surrounded with $Al_{0.35}Ga_{0.65}As$ claddings. The cavity length amounts to 1 mm with as-cleaved facets. The laser has two sections with a ratio of 9 : 1 which are homogeneously biased. The investigated QD laser emits simultaneously on the GS (λ_{GS} = 1168 nm) and ES (λ_{ES} = 1245 nm) for sizeable ranges of currents. The experimental setup is depicted in Fig. 1, the emitted light beam is passed through a collimator and an optical isolator (60 dB isolation), then 1 % of the power is split up to measure the optical spectrum and the intensity temporal traces. The residual

beam is sent to a diffraction grating, which in turn splits the GS and ES emissions into two spatial separated beams. After collimation, the beams present a spatial separation of about 20 mm. A slit allows for the selection of the beam to focus onto the photodetector. The low-noise detection setup consists of a photo diode, a bias-tee and an amplifier. The generated signal by the photo diode is split into an AC and DC part via the bias-tee. The DC part (optical power) is measured with an amperometer, the AC part is amplified and measured by an electrical spectrum analyzer (ESA). The set-up is build in an electrically shielded box to avoid any spurious signals.

To quantify the noise of lasers, the relative intensity noise (RIN) is commonly calculated:

$$RIN = \langle \delta I^2_{Photo}(t) \rangle / \langle I_{Photo}(t) \rangle^2 \quad \textbf{(1)}$$

where $I_{Photo}(t)$ is the photo current of the measured laser output power, the notation $\langle \cdot \rangle$ indicates the temporal average. Thus $\langle I_{Photo}(t) \rangle$ accounts for the DC component of the optical power and $\delta I_{Photo}(t) = I_{Photo}(t) - \langle I_{Photo}(t) \rangle$ refers to its AC component [30, 31].

However, to ensure a correct comparison of the GS and ES emission with the total emission, the optical DC component has to be neglected. This results from the fact that the total emission has approximately double the output power as the GS or ES emission and would artificially reduce the total RIN compared to the GS and ES RIN. For the sake of a correct comparison we therefore disregard the DC component and study only the AC fluctuations $\delta I_{Photo}(t)$. In order to experimentally estimate the AC component δI_{Photo}, we compute the noise current I_n as

$$I_n = \frac{1}{B} \int_B \left(\frac{S(f) - S_{dark-noise}(f)}{R \cdot RBW \cdot G} \right)^{\frac{1}{2}} \mathrm{df} \quad \textbf{(2)}$$

where $S(f) - S_{dark-noise}(f)$ is the dark noise corrected spectral power density, R is the load resistance (50 Ω), RBW the resolution band width of the ESA (100 kHz), G the amplifier gain (36 dB) and B is the spectral integration interval in the range of 25 MHz to 30 MHz [32]. The measurements of $I_{n,tot}$ of the GS+ES emission are performed without beam blocker letting both beams to be focused onto the detector. The value of I_n associated to the GS ($I_{n,GS}$) and to the ($I_{n,ES}$) are measured individually. The GS beam passes a slit and impinges onto the detector while blocking the ES and vice versa.

3. EXPERIMENTAL RESULTS

The Light-Current characteristics of the considered two-states laser for a controlled temperature of −5 °C are reported in Fig. 2(a). This operating condition provides equal optical power for the GS and ES once dual state emission is achieved. With increasing gain current I_{Gain}, first the GS emission threshold is met at 26 mA (■) and the optical power increases up to 60 mA. Then ES starts lasing at 62 mA (◇), where the GS emitted power exhibits a significant reduction. An equal power point is reached at 66 mA (•), where both emissions have an optical power of about 2.8 mW (see also the optical spectrum in the inset). Beyond this point, the optical powers of GS and ES increase similarly with increasing I_{gain}. A total optical power of 16.5 mW is measured at 110 mA, corresponding to 8.1 mW emission for the GS and 8.4 mW for the ES. The measured I_n values are presented in Fig. 2(b) as a function of I_{Gain}. With increasing gain current, the intensity noise of the GS $I_{n,GS}$ (red) and the total intensity noise $I_{n,tot}$ (black) increase up to the GS laser threshold. After a

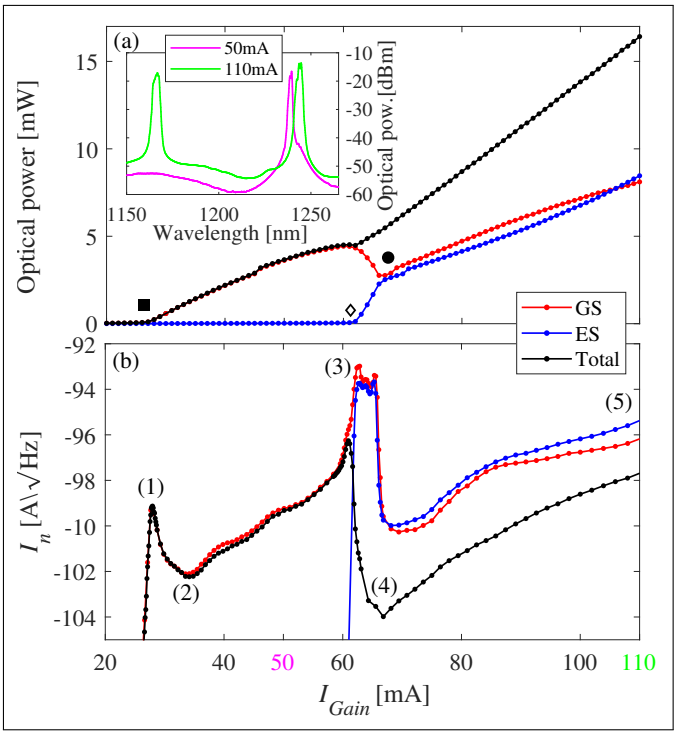

Fig. 2. Experiment: (a) spectrally-resolved GS and ES output power (optical spectra in the inset); (b) noise current I_n for GS, ES and for the total optical power (10 $\log_{10}$ scale). Relevant points indicated by symbols and numbers in brackets are discussed in the text.

first local maximum at 28 mA (1), both decrease to a local minimum at 34 mA (2). The intensity noise of $I_{n,tot}$ and $I_{n,GS}$ increase similarly until the onset of the ES lasing emission, where $I_{n,GS}$ and $I_{n,ES}$ abruptly increase (3). On the other hand, after a significant increment close to the ES threshold, $I_{n,tot}$ decreases down a global minimum at 67 mA (4). For the same current, $I_{n,GS}$ and $I_{n,ES}$ reach as well a minimum. With further increasing gain current all three I_n values start monotonically increasing. From these results we conclude that the values assumed by the noise currents exhibits a non monotonic behavior with maxima $I_{n,tot}$ observable at the GS and ES thresholds ((1) and (3)) remaining always below the noise associated to the single state emission $I_{n,GS}$ and $I_{n,ES}$.

4. SIMULATION MODEL AND RESULTS

In order to reproduce and interpret the experimental evidences reported in the previous section, we performed simulations using a Time Domain Traveling Wave Multi Population Rate Equation Model [33, 34]. The presented model considers N QD sub-groups, regrouping QD with similar sizes, with existence probability G_n and emission peak centered at ω_{nm}, $m = ES, GS$, for a realistic model of gain, refractive index and spontaneous emission spectrum. Using a non excitonic approach, we assume the holes to be in quasi thermal equilibrium; the dynamics of electrons is described using a set of rate equations for each sub-group, following the sketch in Fig. 3(left): the electrons are injected in the barrier, they are then captured in the wetting layer and finally relax in the Second Excited State (SES), the ES and the GS via a cascade processes.

The propagation of the slowly varying components of the

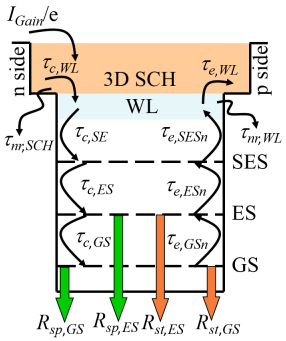

Description	Value
Facet reflectivity R	as cleaved
Confinement factor Γ_{xy}	0.12
Ridge width W	5 µm
Energy gap central group ES	1.054 eV
Energy gap central group GS	0.9879 eV
Homo. linewidth $\hbar\Gamma_{ES/GS}$	14/10 meV
QD density N_D	270 µm^{-2}
QD height h_{QD}	5 nm
Material losses α_i	3.8 cm^{-1}
Dipole matrix element d	6.5×10^{-7} C m
States degeneracy $\mu_{ES/GS}$	4/2
CB relaxation time $\tau_{c,SES/ES/GS}$	3/3/1 ps
QD sub-groups N	51

Fig. 3. (Left) Schematic of the electron dynamics in an exemplary quantum dot sub-group n. (Right) Main parameters used in the simulations; other material parameters used in the model are listed in [35], Table I.

forward and backward electric fields $E^{\pm}(z,t)$ is described by

$$\frac{1}{v_{g0}}\frac{\partial E^{\pm}}{\partial t} \pm \frac{\partial E^{\pm}}{\partial z} = -j\frac{\omega_0}{2c\eta\epsilon_0}\Gamma_{xy}P^{\pm} - \frac{\alpha_i}{2}E^{\pm}(z,t) + S^{\pm} \quad (3)$$

where ω_0 is a reference pulsation, $P^{\pm}(z,t)$ is the macroscopic polarization and $S^{\pm}(z,t)$ is the spontaneous emission noise source; for the definition of other parameters refer to the Table in Fig. 3(right). Assuming a two-level Lorentzian broadening of the QD emission, the macroscopic polarization is calculated as

$$P^{\pm}(z,t) = \frac{N_D}{h_w}\sum_{n=1}^{N}\sum_{m=ES,GS} G_n \mu_m d_m^* p_{nm}^{\pm}(z,t) \quad (4)$$

where $p_{nm}^{\pm}(z,t)$ is the microscopic polarization of the QD sub-group n associated to the emission from the confined level $m = ES, GS$, described as

$$\frac{\partial p_{nm}^{\pm}}{\partial t} = [j(\omega_{nm} - \omega_0) - \Gamma_m]\, p_{nm}^{\pm} + j\frac{d_m}{\hbar}(\rho_{nm}^{e} + \rho_{nm}^{h} - 1)E^{\pm}. \quad (5)$$

In Eq. (5), $\rho_{nm}^{e}(z,t)$ and $\rho_{nm}^{h}(z,t)$ are the occupation probability of electrons and holes in the nm-th state, respectively, whose evolution equations are reported in [33]. The resulting system of differential equations is solved with a finite difference scheme using a time step Δt=10 fs to assure an optical bandwidth about 100 THz to accurately describe the amplified spontaneous emission over frequency bandwidth under exam. To be able to correctly resolve the low frequency fluctuations of the field intensity, long simulation time windows are required; in our case, a numerical integration time window of 250 ns is necessary to simulate a frequency resolution of 4 MHz. To limit the computational time of the simulations, we consider a 200 µm long device, shorter than the one experimentally characterized. From the simulations, we extract the temporal evolution of the power $\tilde{P}_m(t)$ associated to the $m = ES, GS$ emission by filtering the total output power at the laser exit facet $P_{tot}(t) = (1-R)|E^{-}(z=0,t)|^2$ with Hanning windows of suitable -3 dB width B_w centered at the ES and GS emissions ω_m. The simulated DC components of the optical powers versus injected current I_{Gain} are depicted in Fig. 4(a) where we chose B_w = 35 THz. The GS lasing threshold occurs at I_{Gain}=66 mA (■); at I_{Gain}=77 mA (♢) the ES reaches the threshold and we observe, as in the experiment (Fig. 2b), a simultaneous emission from both the QD confined states. The total optical power $\tilde{P}_{tot}$, filtered using the same bandwidth B_w, is plotted in black and increases almost linearly. An equal power

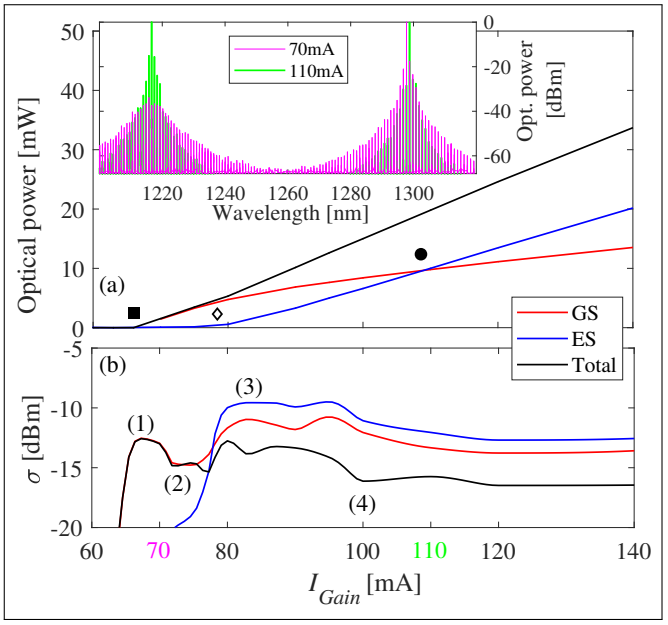

Fig. 4. Simulation: (a) spectrally-resolved GS and ES output power (optical spectra in the inset); (b) standard deviations of the optical powers for GS, ES and for the total power.

point of about 10 mW is reached at I_{Gain}=110 mA (•). After the ES threshold current we observe a reduction in the local derivate of the GS power which is attributed to de-synchronized dynamics of electrons and holes in the QD states [6]. In Fig. 4(b), in analogy with the experimental results presented in Fig. 2(b), we report as a function of the injected current I_{Gain} the standard deviations σ_m of the optical powers $\tilde{P}_m$, with $m = GS, ES, tot$ defined as $\sigma_m = \sqrt{\langle P_m(t) - \langle P_m(t)\rangle\rangle}$ which clearly represents a theoretical estimation of the measured intensity noise current I_n. In agreement with experimental findings presented in Fig. 2(b), our theoretical results show that the noise in the total power exhibits a local maximum at the GS lasing onset (1), then decreases with increasing I_{Gain} (2); it reaches a global maximum close to the threshold for the ES lasing (3) and after this point it remains about 4 dB smaller than the noise of the sole GS or ES emission (4). This dynamical behavior suggests the existence of quasi compensation between the low frequency intensity fluctuations of the GS and ES power. We note that when the noise source is removed both the GS and ES emissions are stable.

The antiphase dynamics is also confirmed by the analysis of the measured and simulated AC components of the power fluctuations. To match the experiments, in this case we filtered the output powers numerical traces using a value of the bandwidth B_w of 35 MHz. In Fig. 5(a) we report the AC fluctuations of $\tilde{P}_m$, $m = GS, ES, tot$ for a fixed current injection of I_{Gain} = 110 mA that corresponds to an equal power point. In Fig. 5(b) we plot the phase differences between the corresponding Fourier components amplitudes of the GS and ES time traces in Fig. 5(a) that are all close to π, but not exactly equal as it should be in case of perfect antiphase dynamics. The experimental time-traces are depicted in Fig. 5(c) and qualitatively confirm the numerical results. Specifically, they reveal that the power fluctuations of the total emission are smaller than those associated with the single emission states, but also that the latter only compensate to a certain degree. This partial compensation can be attributed to the non instantaneous dynamics of the electrons density trough

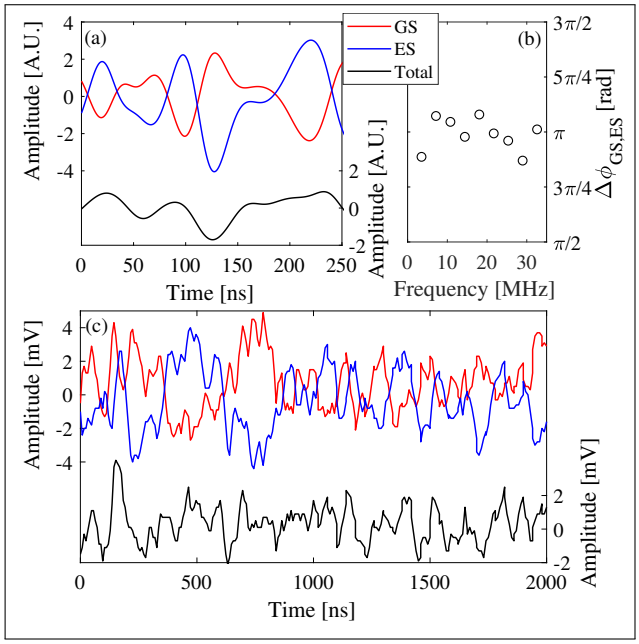

Fig. 5. Simulation: (a) Spectrally-resolved GS and ES and total optical power fluctuations filtered with a bandwidth B_w= 35 MHz and (b) phase difference $\Delta\phi_{GS,ES}$ between the corresponding Fourier components amplitudes of the GS and ES emissions. Experiment: (c) Noise current for GS, ES, and the total optical power.

which the ES and GS emission are coupled, in analogy to what reported in the study of the two modes dynamics in multi transverse or longitudinal modes semiconductor lasers [36, 37].

5. CONCLUSION

In this work the amplitude stability of an InAs/InGaAs quantum dot laser has been investigated both experimentally and by numerical modeling. Experimentally, a reduction in power fluctuations up to 4 dB is found when GS and ES emit simultaneously as compared to the case of single GS or ES emission. This stability is also studied by spectrally resolved GS and ES time-signal analysis. By means of numerical simulations we explained this phenomenon and qualitatively reproduce its trend with the laser biasing conditions. We identify the coupling of GS and ES emissions trough the cascade carrier relaxation as the underlying physical mechanism leading to a quasi antiphase dynamics and we ascribed the non perfect GS and ES emissions compensation to the non instantaneous carriers dynamics (finite relaxation times).

ACKNOWLEDGEMENT

The authors would like to thank L. Drzewietzki, W. Elsäßer and S. Hartmann from TU Darmstadt and M. Virte of VUB, Brussels, Belgium for fruitful discussions, I. Krestnikov and his team from Innolume GmbH, Dortmund, Germany, for growing the excellent QD wafer and W. Rök from Technische Universität Darmstadt for excellent technical assistance.

REFERENCES

1. M. Grundmann and D. Bimberg, Phys. Rev. B **55**, 9740 (1997).
2. M. Grundmann, A. Weber, K. Goede, V. M. Ustinov, A. E. Zhukov, N. N. Ledentsov, P. S. Kop'ev, and Z. I. Alferov, Appl. Phys. Lett. **4** (2000).
3. E. A. Viktorov, P. Mandel, Y. Tanguy, J. Houlihan, and G. Huyet, Applied Physics Letters **87**, 053113 (2005).
4. E. A. Viktorov, M. A. Cataluna, L. O'Faolain, T. F. Krauss, W. Sibbett, E. U. Rafailov, and P. Mandel, App. Phys. Lett. **90**, 121113 (2007).
5. K. Veselinov, F. Grillot, C. Cornet, J. Even, A. Bekiarski, M. Gioannini, and S. Loualiche, IEEE J. Quantum. Electron. **43**, 810 (2007).
6. M. Gioannini, J. Appl. Phys. **111**, 043108 (2012).
7. T. Xu, M. Rossetti, P. Bardella, and I. Montrosset, IEEE J. Quantum Electron. **48**, 1193 (2012).
8. V. V. Korenev, A. V. Savelyev, A. E. Zhukov, A. V. Omelchenko, and M. V. Maximov, Semiconductors **47**, 1397 (2013).
9. A. Röhm, B. Lingnau, and K. Lüdge, IEEE J. Quantum Electron. **51**, 1 (2015).
10. V. V. Korenev, A. V. Savelyev, M. V. Maximov, F. I. Zubov, Y. M. Shernyakov, and A. E. Zhukov, J. Phys. **917**, 052001 (2017).
11. A. Markus, J. X. Chen, C. Paranthoen, A. Fiore, C. Platz, and O. Gauthier-Lafaye, Appl. Phys. Lett. **82**, 1818 (2003).
12. M. Sugawara, N. Hatori, H. Ebe, M. Ishida, Y. Arakawa, T. Akiyama, K. Otsubo, and Y. Nakata, J. Appl. Phys. **97** (2005).
13. A. Markus, M. Rossetti, V. Calligari, D. Chek-Al-Kar, J. X. Chen, A. Fiore, and R. Scollo, J. App. Phys. **100** (2006).
14. M. A. Cataluna, W. Sibbett, D. A. Livshits, J. Weimert, A. R. Kovsh, and E. U. Rafailov, Appl. Phys. Lett. **89**, 081124 (2006).
15. Q. Cao, S. F. Yoon, C. Z. Tong, C. Y. Ngo, C. Y. Liu, R. Wang, and H. X. Zhao, Appl. Phys. Lett. **191101** (2009).
16. J. Lee and D. Lee, J. Korean Phys. Soc. **58**, 239 (2011).
17. M. V. Maximov, Y. M. Shernyakov, F. I. Zubov, A. E. Zhukov, N. Y. Gordeev, V. V. Korenev, A. V. Savelyev, and D. A. Livshits, Semicond. Sci. Technol. **28**, 105016 (2013).
18. D. Arsenijevic, A. Schliwa, H. Schmeckebier, M. Stubenrauch, M. Spiegelberg, D. Bimberg, V. Mikhelashvili, and G. Eisenstein, Applied Physics Letters **104**, 181101 (2014).
19. S. Breuer, M. Rossetti, W. Elsässer, L. Drzewietzki, P. Bardella, I. Montrosset, M. Krakowski, and M. Hopkinson, Appl. Phys. Lett. **97** (2010).
20. S. Breuer, M. Rossetti, I. Montrosset, M. Krakowski, M. Hopkinson, and W. Elsässer, IEEE J. Sel. Top. Quantum Electron. **19**, 1 (2013).
21. E. A. Viktorov, P. Mandel, I. O'Driscoll, O. Carroll, G. Huyet, J. Houlihan, and Y. Tanguy, Optics Letters **31**, 2302 (2006).
22. I. V. Koryukin, Phys. Rev. A **92**, 043840 (2015).
23. M. Gioannini, M. Dommermuth, L. Drzewietzki, I. Krestnikov, D. Livshits, M. Krakowski, and S. Breuer, Opt. Express **22**, 23402 (2014).
24. Y. Tanguy, J. Houlihan, G. Huyet, E. A. Viktorov, and P. Mandel, Phys. Rev. Lett. **96**, 053902 (2006).
25. L. Capua, V. Rozenfeld, V. Mikhelashvili, G. Eisenstein, M. Kuntz, M. Laemmlin, and D. Bimberg, Opt. Express **15**, 5388 (2007).
26. A. Gubenko, I. Krestnikov, D. Livshits, S. Mikhrin, A. Kovsh, L. West, C. Bornholdt, N. Grote, and A. Zhukov, Electron. Lett. **43**, 1430 (2007).
27. H. Lin, H. L. Tang, H. C. Cheng, and H. L. Chen, IEEE J. Lightw. Technol. **30**, 331 (2012).
28. D. Gready, G. Eisenstein, C. Gilfert, V. Ivanov, and J. P. Reithmaier, IEEE Photon. Technol. Lett. **24**, 809 (2012).
29. R. Pawlus, S. Breuer, and M. Virte, Optics Letters **42**, 4259 (2017).
30. R. Müller, Rauschen (Springer, Berlin, 1979).
31. K. Petermann, Laser diode modulation and noise (Advances in Optoelectronics 3, Kluwer Academic Publishers, 1988).
32. T. Gensty, W. Elsäßer, and C. Mann, Optics Express **13**, 2032 (2005).
33. P. Bardella, M. Rossetti, and I. Montrosset, IEEE J. Sel. Top. Quantum Electron. **15**, 785 (2009).
34. M. Rossetti, P. Bardella, and I. Montrosset, IEEE J. Quantum Electron. **47**, 139 (2011).
35. M. Gioannini, P. Bardella, and I. Montrosset, IEEE J. Sel. Top. Quantum Electron. **21**, 1900811 (2015).
36. A. M. Yacomotti, L. Furfaro, X. Hachair, F. Pedaci, M. Giudici, J. Tredicce, J. Javaloyes, S. Balle, E. A. Viktorov, and P. Mandel, Phys. Rev. A **69**, 053816 (2004).
37. L. Columbo, M. Brambilla, M. Dabbicco, and G. Scamarcio, Opt. Express **20**, 6286 (2012).

FULL REFERENCES

1. M. Grundmann and D. Bimberg, "Theory of random population for quantum dots," Phys. Rev. B **55**, 9740 (1997).
2. M. Grundmann, A. Weber, K. Goede, V. M. Ustinov, A. E. Zhukov, N. N. Ledentsov, P. S. Kop'ev, and Z. I. Alferov, "Midinfrared emission from near-infrared quantum-dot lasers," Appl. Phys. Lett. **4** (2000).
3. E. A. Viktorov, P. Mandel, Y. Tanguy, J. Houlihan, and G. Huyet, "Electron-hole asymmetry and two-state lasing in quantum dot lasers," Applied Physics Letters **87**, 053113 (2005).
4. E. A. Viktorov, M. A. Cataluna, L. O'Faolain, T. F. Krauss, W. Sibbett, E. U. Rafailov, and P. Mandel, "Dynamics of a two-state quantum dot laser with saturable absorber," App. Phys. Lett. **90**, 121113 (2007).
5. K. Veselinov, F. Grillot, C. Cornet, J. Even, A. Bekiarski, M. Gioannini, and S. Loualiche, "Analysis of the double laser emission occurring in 1.55-µm inas–inp (113)b quantum-dot lasers," IEEE J. Quantum. Electron. **43**, 810–816 (2007).
6. M. Gioannini, "Ground-state power quenching in two-state lasing quantum dot lasers," J. Appl. Phys. **111**, 043108 (2012).
7. T. Xu, M. Rossetti, P. Bardella, and I. Montrosset, "Simulation and analysis of dynamic regimes involving ground and excited state transitions in quantum dot passively mode-locked lasers," IEEE J. Quantum Electron. **48**, 1193–1202 (2012).
8. V. V. Korenev, A. V. Savelyev, A. E. Zhukov, A. V. Omelchenko, and M. V. Maximov, "Effect of carrier dynamics and temperature on two-state lasing in semiconductor quantum dot lasers," Semiconductors **47**, 1397–1404 (2013).
9. A. Röhm, B. Lingnau, and K. Lüdge, "Understanding ground-state quenching in quantum-dot lasers," IEEE J. Quantum Electron. **51**, 1–11 (2015).
10. V. V. Korenev, A. V. Savelyev, M. V. Maximov, F. I. Zubov, Y. M. Shernyakov, and A. E. Zhukov, "The effect of p-doping on multi-state lasing in inas/ingaas quantum dot lasers for different cavity lengths," J. Phys. **917**, 052001 (2017).
11. A. Markus, J. X. Chen, C. Paranthoen, A. Fiore, C. Platz, and O. Gauthier-Lafaye, "Simultaneous two-state lasing in quantum-dot lasers," Appl. Phys. Lett. **82**, 1818–1820 (2003).
12. M. Sugawara, N. Hatori, H. Ebe, M. Ishida, Y. Arakawa, T. Akiyama, K. Otsubo, and Y. Nakata, "Spectra of 1.3 μm self-assembled inas/gaas quantum-dot lasers: Homogeneous broadening of optical gain under current injectionmodeling room-temperature lasing," J. Appl. Phys. **97** (2005).
13. A. Markus, M. Rossetti, V. Calligari, D. Chek-Al-Kar, J. X. Chen, A. Fiore, and R. Scollo, "Two-state switching and dynamics in quantum dot two-section lasers," J. App. Phys. **100** (2006).
14. M. A. Cataluna, W. Sibbett, D. A. Livshits, J. Weimert, A. R. Kovsh, and E. U. Rafailov, "Stable mode locking via ground- or excited-state transitions in a two-section quantum-dot laser," Appl. Phys. Lett. **89**, 081124 (2006).
15. Q. Cao, S. F. Yoon, C. Z. Tong, C. Y. Ngo, C. Y. Liu, R. Wang, and H. X. Zhao, "Two-state competition in 1.3μm multilayer inas/ingaas quantum dot lasers," Appl. Phys. Lett. **191101** (2009).
16. J. Lee and D. Lee, "Double-state lasing from semiconductor quantum dot laser diodes caused by slow carrier relaxation," J. Korean Phys. Soc. **58**, 239 (2011).
17. M. V. Maximov, Y. M. Shernyakov, F. I. Zubov, A. E. Zhukov, N. Y. Gordeev, V. V. Korenev, A. V. Savelyev, and D. A. Livshits, "The influence of p-doping on two-state lasing in inas/ingaas quantum dot lasers," Semicond. Sci. Technol. **28**, 105016 (2013).
18. D. Arsenijevic, A. Schliwa, H. Schmeckebier, M. Stubenrauch, M. Spiegelberg, D. Bimberg, V. Mikhelashvili, and G. Eisenstein, "Comparison of dynamic properties of ground- and excited-state emission in p-doped inas/gaas quantum-dot lasers," Applied Physics Letters **104**, 181101 (2014).
19. S. Breuer, M. Rossetti, W. Elsässer, L. Drzewietzki, P. Bardella, I. Montrosset, M. Krakowski, and M. Hopkinson, "Reverse-emission-state-transition mode locking of a two-section inas/ingaas quantum dot laser," Appl. Phys. Lett. **97** (2010).
20. S. Breuer, M. Rossetti, I. Montrosset, M. Krakowski, M. Hopkinson, and W. Elsässer, "Dual-state absorber-photocurrent characteristics and bistability of two-section quantum-dot lasers," IEEE J. Sel. Top. Quantum Electron. **19**, 1–9 (2013).
21. E. A. Viktorov, P. Mandel, I. O'Driscoll, O. Carroll, G. Huyet, J. Houlihan, and Y. Tanguy, "Low-frequency fluctuations in two-state quantum dot lasers," Optics Letters **31**, 2302–2304 (2006).
22. I. V. Koryukin, "Relaxation oscillations in a semiconductor quantum-dot laser," Phys. Rev. A **92**, 043840 (2015).
23. M. Gioannini, M. Dommermuth, L. Drzewietzki, I. Krestnikov, D. Livshits, M. Krakowski, and S. Breuer, "Two-state semiconductor laser self-mixing velocimetry exploiting coupled quantum-dot emission-states: experiment, simulation and theory," Opt. Express **22**, 23402–23414 (2014).
24. Y. Tanguy, J. Houlihan, G. Huyet, E. A. Viktorov, and P. Mandel, "Synchronization and clustering in a multimode quantum dot laser," Phys. Rev. Lett. **96**, 053902 (2006).
25. L. Capua, V. Rozenfeld, V. Mikhelashvili, G. Eisenstein, M. Kuntz, M. Laemmlin, and D. Bimberg, "Direct correlation between a highly damped modulation response and ultra low relative intensity noise in inas/gaas quantum dot laser," Opt. Express **15**, 5388–5393 (2007).
26. A. Gubenko, I. Krestnikov, D. Livshits, S. Mikhrin, A. Kovsh, L. West, C. Bornholdt, N. Grote, and A. Zhukov, "Error-free 10 gbit/s transmission using individual fabry-perot modes of low-noise quantum-dot laser," Electron. Lett. **43**, 1430–1431 (2007).
27. H. Lin, H. L. Tang, H. C. Cheng, and H. L. Chen, "Analysis of relative intensity noise spectra for uniformly and chirpily stacked inas-ingaas-gaas quantum dot lasers," IEEE J. Lightw. Technol. **30**, 331–336 (2012).
28. D. Gready, G. Eisenstein, C. Gilfert, V. Ivanov, and J. P. Reithmaier, "Highspeed low-noise inas/inalgaas/inp 1.55-μm quantum-dot lasers," IEEE Photon. Technol. Lett. **24**, 809–811 (2012).
29. R. Pawlus, S. Breuer, and M. Virte, "Relative intensity noise reduction in a dual-state quantum-dot laser by optical feedback ," Optics Letters **42**, 4259–4262 (2017).
30. R. Müller, Rauschen (Springer, Berlin, 1979).
31. K. Petermann, Laser diode modulation and noise (Advances in Optoelectronics 3, Kluwer Academic Publishers, 1988).
32. T. Gensty, W. Elsäßer, and C. Mann, "Intensity noise properties of quantum cascade lasers," Optics Express **13**, 2032 (2005).
33. P. Bardella, M. Rossetti, and I. Montrosset, "Modeling of broadband chirped quantum-dot super-luminescent diodes," IEEE J. Sel. Top. Quantum Electron. **15**, 785–791 (2009).
34. M. Rossetti, P. Bardella, and I. Montrosset, "Time-domain travelling-wave model for quantum dot passively mode-locked lasers," IEEE J. Quantum Electron. **47**, 139–150 (2011).
35. M. Gioannini, P. Bardella, and I. Montrosset, "Time-domain traveling-wave analysis of the multimode dynamics of quantum dot fabry-perot lasers," IEEE J. Sel. Top. Quantum Electron. **21**, 1900811 (2015).
36. A. M. Yacomotti, L. Furfaro, X. Hachair, F. Pedaci, M. Giudici, J. Tredicce, J. Javaloyes, S. Balle, E. A. Viktorov, and P. Mandel, "Dynamics of multimode semiconductor lasers," Phys. Rev. A **69**, 053816 (2004).
37. L. Columbo, M. Brambilla, M. Dabbicco, and G. Scamarcio, "Self-mixing in multi-transverse mode semiconductor lasers: model and potential application to multi-parametric sensing," Opt. Express **20**, 6286–6305 (2012).